SPECT Imaging of Normal Subjects with Technetium-99m-HMPAO and Technetium-99m-ECD

Masamichi Koyama, Ryuta Kawashima, Hiroshi Ito, Shuichi Ono, Kazunori Sato, Ryoui Goto, Shigeo Kinomura, Seiro Yoshioka, Tachio Sato and Hiroshi Fukuda

Department of Nuclear Medicine and Radiology, Division of Brain Sciences, Institute of Development, Aging and Cancer, Tohoku University, Sendai, Japan

Technetium-99m-HMPAO and ^{99m}Tc-ECD have been used for regional cerebral blood flow (rCBF) studies using SPECT. However, details of the normal perfusion patterns of these agents still remain to be clarified. HMPAO-SPECT and ECD-SPECT images of normal individuals were investigated using an anatomical standardization technique. **Methods:** Twenty healthy subjects participated in this study. In 10 of these, regional cerebral perfusion was measured with HMPAO, and in the other 10, ECD was used. All SPECT images were globally normalized to 50 counts/voxel, and then, each SPECT image was transformed into a standard brain anatomy format with the aid of x-ray CT of each subject and a computerized human brain atlas system (HBA). Mean and s.d. images for each tracer were calculated on a voxel-by-voxel basis. For comparison of these SPECT images with blood flow, rCBF images were generated using PET in a separate group of 10 healthy male subjects during an eyes-closed resting state. The PET images were globally normalized to 50 ml/100 g/min and anatomically standardized using each subject's MRI and the HBA for the SPECT images. **Results:** In the HMPAO-SPECT images, relatively high radioactivities were observed in the basal ganglia and cerebellum. In the ECD-SPECT images, high levels were observed in the medial aspect of the occipital lobe. These regions with high radioactivity were not apparent in the rCBF-PET images. **Conclusion:** While both HMPAO and ECD have been used to investigate rCBF, their perfusion patterns differ from rCBF-PET images. This presumably reflects differences in the mechanism of accumulation of each agent in the brain. For clinical diagnoses, these patterns must be taken into consideration.

Key Words: technetium-99m-HMPAO; technetium-99m-ECD; SPECT; anatomical standardization

J Nucl Med 1997; 38:587–592

Technetium-99m-hexamethylpropylene amine oxime (HMPAO) has been used for cerebral perfusion studies with SPECT due to its large first-pass extraction fraction and high affinity for the brain (*1*). Recently, a neutral lipophilic complex, ^{99m}Tc-ethyl cysteinate dimer (ECD) was introduced as a tracer for cerebral perfusion imaging, which also showed high cerebral retention (*2,3*). The clinical usefulness of HMPAO and ECD has been stressed for cerebrovascular disease (*4,5*), neurodegenerative changes (*6*), tumors (*7*), epilepsy (*8*), depression (*9*) and trauma (*10*). However, the cerebral perfusion patterns of each of these agents in normal subjects still remain unclear. Therefore, this study was performed with the specific aim of determining normal cerebral perfusion patterns from HMPAO and ECD images and comparing these with regional cerebral flow (rCBF) images gained from PET. For this purpose, an anatomical standardization technique which can describe the characteristics of RI accumulation pattern of group mean images (*9*) was applied using the new computerized human brain atlas (HBA) system of Roland et al. (*11*). Brain images of subjects were thereby transformed into the same standard anatomical form by using both linear and nonlinear parameters.

Received Apr. 12, 1996; revision accepted Jul. 22, 1996.

For correspondence or reprints contact: Ryuta Kawashima, MD, Dept. of Nuclear Medicine and Radiology, Division of Brain Sciences, Institute of Development, Aging and Cancer, Tohoku University, 4–1 Seiryo-Machi, Aoba-Ku, Sendai, Japan 980.

MATERIALS AND METHODS

Subjects

Twenty subjects participated in this study. In 10 patients (7 men, 3 women; age range 34–63 yr, mean age 46 yr), regional cerebral perfusion was measured with HMPAO (984 ± 17 MBq), and in the other 10 patients (8 men, 2 women; age range 36–62 yr; mean age 46 yr), ECD (792 ± 95 MBq) was used. All subjects were right handed as assessed by the H.N. Handedness Inventory (*12*). None had any prior medical history or present illness. All subjects had normal x-ray CT scans taken on the same day as the SPECT measurement. Written informed consent was obtained from each subject according to the declaration of Helsinki, 1975.

SPECT Study

Each SPECT scan was performed 5–10 min after injection of HMPAO or ECD. All subjects were lying in a supine position with their eyes closed from the time of the injection through to completion of the SPECT measurement.

The position of the head was adjusted using three-dimensional laser alignment beams of SPECT apparatus. The orbitomeatal (OM) line was aligned with the horizontal beam, the head symmetrically positioned about the midsagittal plane. To minimize differences in the alignment between the x-ray CT and SPECT, line markers were drawn directly on subject's faces.

A four-head, rotating gamma SPECT camera with in-plane and axial resolutions of 8-mm FWHM was used for all measurements (*13*). The camera was fitted with a low-energy, high-resolution (LEHR) collimator. The SPECT scan protocol acquired 64 projections at 20 sec (20 sec × four-head camera = total 80 sec) per projection with 360° rotation of the camera. Image reconstruction was performed by filtered backprojection using a Butterworth filter resulting in a spatial resolution of 10.6 mm (*14*). Attenuation correction was made numerically by assuming the object shape to be an ellipse for each slice and the attenuation coefficient to be uniform (0.1 cm^{-1}) (*15,16*). Correction for scattered photons was not performed. Axial image slices were set up parallel to the OM line and obtained for 8-mm intervals through the whole brain.

PET Study

PET studies were performed on 10 healthy male subjects (aged 20–32 yr). All were right handed except for one ambidextrous person. All subjects had normal MR images and blood laboratory examination.

TABLE 1
Mean (s.d.) CBF and Regional Distribution of Normalized Radioactivities

Region	Volume (mm^3)	PET-rCBF (ml/100 g/min)	HMPAO (counts/voxel)	ECD (counts/voxel)
Brain stem				
Pons	6060	na	52.9 (6.2)	47.4 (7.4)
Midbrain†	7320	55.6 (6.5)	54.8 (5.1)	48.5 (6.6)
Cerebellum				
Vermis	1850	59.3 (6.6)	70.7 (4.5)	69.2 (6.3)
rt hemisphere	19840	60.3 (6.5)	65.2 (6.5)	62.9 (7.3)
lt hemisphere	19420	63.1 (6.7)	67.2 (5.4)	64.8 (7.1)
Central gray matter				
rt caudate†	1230	63.9 (7.0)	66.6 (5.4)	59.1 (6.5)
lt caudate	1370	56.8 (6.3)	61.3 (6.9)	56.0 (6.7)
rt putamen†	2220	75.0 (8.1)	71.9 (3.8)	66.0 (6.4)
lt putamen†	2260	74.6 (8.5)	70.9 (4.6)	64.3 (6.2)
rt thalamus†	2800	62.1 (7.1)	63.4 (5.0)	55.3 (6.9)
lt thalamus†	2770	70.2 (7.7)	63.4 (5.8)	54.7 (7.0)
Limbic system				
rt ant cingulate	1050	67.7 (7.8)	57.7 (6.6)	55.3 (8.2)
lt ant cingulate	1010	73.2 (7.8)	52.1 (6.7)	50.9 (7.0)
rt parahippo gy	1950	50.2 (5.7)	58.4 (7.2)	52.7 (5.9)
lt parahippo gy	2380	54.2 (5.8)	52.7 (6.3)	51.3 (8.1)
Temporal cortex				
rt sup temporal gy	2160	68.7 (6.9)	64.1 (4.5)	59.7 (6.2)
lt sup temporal gy†	2160	68.7 (7.1)	61.6 (6.2)	54.1 (7.5)
rt mid temporal gy	1450	63.9 (7.0)	62.6 (4.6)	59.1 (5.2)
lt mid temporal gy	1940	56.0 (6.1)	59.2 (4.9)	56.0 (7.5)
rt inf temporal gy	2450	53.1 (6.5)	57.3 (5.4)	52.9 (8.5)
lt inf temporal gy	2880	48.6 (5.6)	55.3 (7.1)	51.1 (7.7)
Insular cortex				
rt insula	2920	86.5 (8.7)	66.0 (5.0)	62.0 (5.9)
lt insula	2990	82.9 (8.3)	62.9 (6.3)	58.0 (7.0)
Frontal cortex				
rt sup frontal gy	1660	64.5 (7.1)	60.9 (5.5)	56.5 (7.3)
lt sup frontal gy	1510	60.6 (6.1)	56.9 (7.8)	54.7 (8.1)
rt mid frontal gy	2160	69.1 (7.5)	62.1 (6.3)	57.7 (6.5)
lt mid frontal gy	2160	65.4 (6.8)	60.7 (7.2)	54.0 (11.2)
rt inf frontal gy	1280	68.2 (7.4)	59.0 (4.0)	54.3 (6.0)
lt inf frontal gy	1140	66.2 (7.2)	59.3 (5.4)	52.1 (10.4)
rt precentral gy	1440	74.2 (7.8)	59.2 (4.1)	55.6 (5.5)
lt precentral gy	1440	72.7 (7.9)	57.2 (5.5)	51.9 (6.0)
Parietal cortex				
rt postcentral gy	1440	64.0 (6.8)	57.1 (4.0)	56.2 (6.4)
lt postcentral gy	1440	72.1 (7.5)	58.3 (4.4)	54.7 (5.8)
rt precuneus	2160	71.2 (7.5)	66.4 (4.7)	69.8 (6.8)
lt precuneus	2160	77.9 (8.2)	68.1 (4.9)	71.8 (5.4)
Occipital cortex				
rt lingual gy	2160	67.2 (7.4)	67.5 (5.2)	72.9 (6.8)
lt lingual gy‡	2160	74.9 (7.8)	67.7 (5.5)	75.6 (6.5)
rt cuneus	2160	63.1 (6.7)	66.8 (5.6)	71.1 (6.9)
lt cuneus	2160	71.0 (7.2)	65.0 (6.0)	70.4 (5.6)
rt post occipital area	1890	53.8 (5.7)	59.7 (6.7)	63.3 (8.5)
lt post occipital area	2430	58.9 (6.3)	59.1 (5.8)	63.7 (7.4)
rt lat occipital area	2090	51.1 (6.2)	53.4 (7.4)	54.1 (6.0)
lt lat occipital area	2030	53.2 (5.8)	57.8 (4.7)	56.9 (5.2)
Gray matter	67350	64.1 (7.0)	61.5 (5.6)	59.3 (6.9)
White matter	12690	24.2 (3.7)	43.0 (4.8)	38.9 (5.8)

* White matter includes six circular ROIs (8.3 mm in radius), which are drawn on the anterior and posterior paraventricular deep white matter and the semioval center of the bilateral hemisphere.

†Significantly higher in HMPAO compared with ECD ($p < 0.05$, t-test).

‡Significantly higher in ECD compared with HMPAO ($p < 0.01$, t-test).

rt, lt, sup, mid, inf, lat, ant, post, parahippo and gy indicate right, left, superior, middle, inferior, lateral, anterior, posterior, parahippocampal and gyrus, respectively. na = not available in PET study because of its scan range.

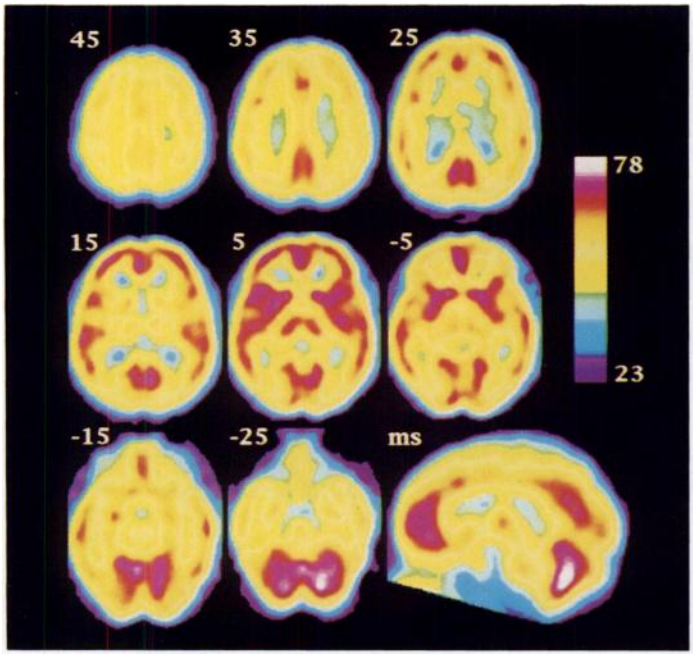

FIGURE 1. Mean images of anatomically standardized ^{99m}Tc-HMPAO SPECT. All slices except the bottom right ones are parallel to the horizontal plane through the AC-PC line (top left: 45 mm above the AC-PC line and after pictures at 10-mm interslice intervals). The anterior is at the top of the image and the subject's right is at the left. The mid-sagittal section is shown at bottom right (ms). The anterior is at the left of the image. Images were thresholded at the upper and lower limits of 78 and 23 counts, respectively.

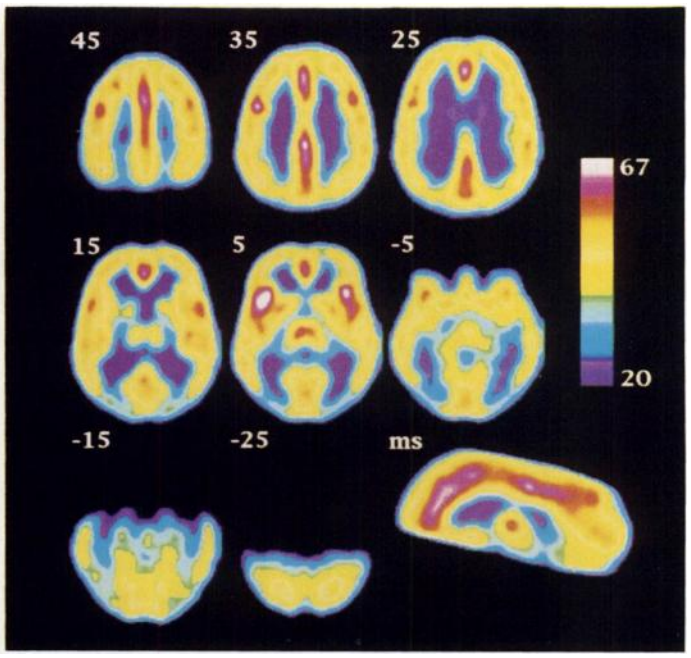

FIGURE 3. Mean images of anatomically standardized PET-CBF images, which were globally normalized to 50 ml/100 g/min and spatially smoothed. The images were thresholded at the upper and lower limits of 67 and 20 ml/100 g/min, respectively. The format is the same as in Figure 1.

From the injection through the data collection, each subject rested comfortably in a supine position having his head fixed in a stereotaxic helmet (*17*) with his eyes closed. Each subject had a catheter placed into the right brachial vein for tracer administration and another inserted, under local anesthesia, into the left radial artery for measurement of arterial radioisotope activity.

PET Imaging

The rCBF was measured with an eight-ring, 15-slice PET camera having an in-plane spatial resolution of 4.5 mm and an interslice distance of 6.5 mm. Approximately 2.6 GBq ^{15}O-butanol were injected intravenously as a bolus. The arterial input function was continuously monitored, and the rCBF was calculated on the basis of the data from 0–80 sec as previously described (*18*). Measured attenuation corrections were made with the ratio of counts in blank and transmission scans obtained ^{68}Ge source. The images were reconstructed with the aid of a 4-mm Hanning filter.

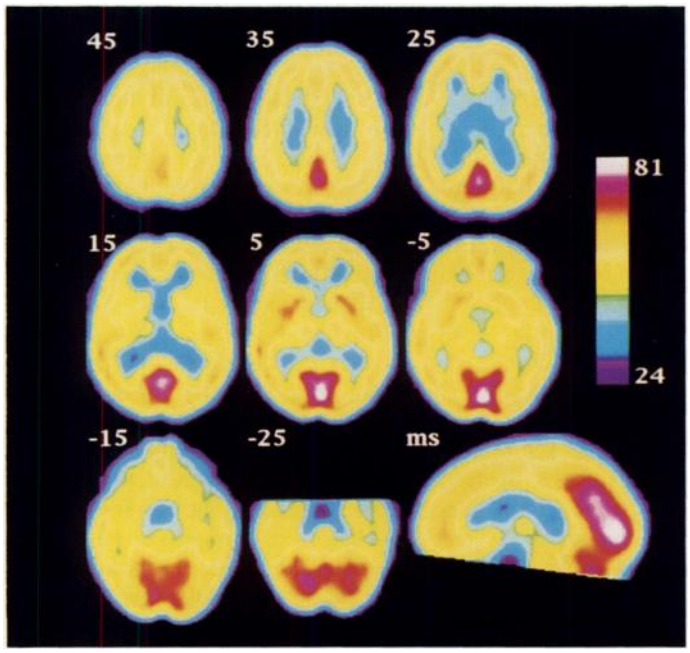

FIGURE 2. Mean images of anatomically standardized ^{99m}Tc-ECD SPECT. Images were thresholded at the upper and lower limits of 81 and 24 counts, respectively. The format is the same as in Figure 1.

Data Analysis

All SPECT images were globally normalized with averaging of whole brain radioactivity counts to 50 counts/voxel and then transformed into the standard brain size and shape using the HBA system as previously described (*11*). Briefly, the anatomical structures of the computerized standard brain atlas were fitted interactively to each subject's x-ray CT image, using both linear and nonlinear parameters. Special attention was given to accurate fitting of the brain contours, lateral ventricles, basal ganglia, thalamus, central sulcus and the lateral sulcus in all subjects. These parameters were subsequently used to transform each subject's SPECT image into the standard atlas form. After the anatomical standardization procedure, all subjects' SPECT images had the same brain anatomical format. The anatomical standardization process does not show any significant change of the counts within the brain (*18*). Then, mean and s.d. images for each tracer were calculated on a voxel-by-voxel basis.

Regions of interest (ROI) for anatomical structures shown in Table 1 were manually outlined on the standard brain atlas of the HBA by both a participating neuroradiologist and the first author of this article. The population mean (s.d.) relative RI concentration was then calculated for each ROI.

The PET images were globally normalized to 50 ml/100 g/min and anatomically standardized using HBA and each subject's MRI in the same way as for SPECT. Then mean (s.d.) rCBF images were calculated voxel-by-voxel. The same ROIs were reproduced on the rCBF-PET images as well. Finally, rCBF-PET images were smoothed with a three-dimensional Gausian filter (8 mm FWHM). This allowed visual comparison of rCBF-PET with HMPAO-SPECT and ECD-SPECT images.

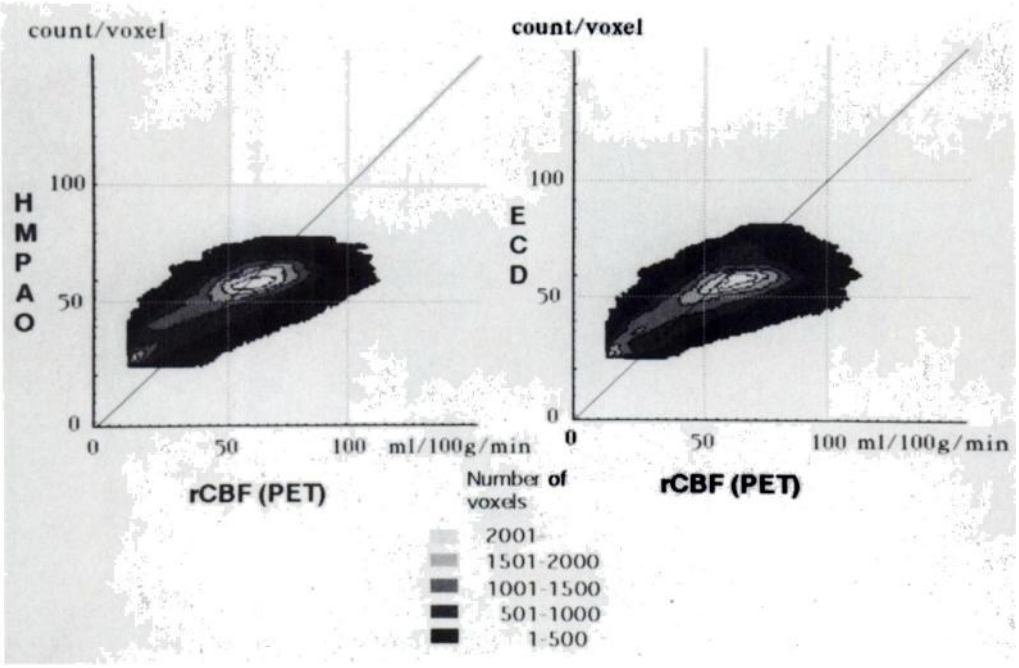

FIGURE 4. Scatterplots of the overall correlation between radioactivitiy of HMPAO (left) and ECD (right) SPECT and rCBF measured with ^{15}O-butanol PET represented in contours according to the voxel numbers. Curvilinear relationships are demonstrated with underestimation of high flow by SPECT.

Statistical Analysis

To compare HMPAO with ECD in each ROI, two sample Student's t-tests were used. To compare these tracers in grouped ROIs, two-way ANOVA (tracer by region) was used.

The correction for multiple comparisons was done by Dunnett's method (*19*) to evaluate the statistical significance of differences between the SPECT images and the PET images.

RESULTS

Figures 1 and 2 show mean SPECT images with HMPAO and ECD, respectively. In the HMPAO-SPECT images, relatively high radioactivities were observed in the basal ganglia and the cerebellum. In the ECD-SPECT images, this was the case with the medial aspect of the occipital lobe. Figure 3 shows mean rCBF-PET images. Relatively high levels were observed in the insula and the cingulate gyrus but not in the basal ganglia and cerebellum, as with HMPAO, or the medial aspect of the occipital lobe, as with ECD.

Table 1 shows mean rCBF value measured with ^{15}O-butanol PET and mean radioactivity of HMPAO and ECD in each ROI. Mean normalized radioactivity in the midbrain, right caudate, bilateral putamen, bilateral thalamus and left superior temporal gyrus were found to be significantly higher with HMPAO as compared to the ECD case (Student's t-test, $p < 0.01$ for bilateral thalamus, and $p < 0.05$ for the other ROIs). On the other hand, ECD gave significantly higher radioactivities than HMPAO in the left lingual gyrus (Student's t-test, $p < 0.01$). In the medial aspect of the parieto-occipital region (that is the precuneus, cuneus and lingual gyrus), ECD demonstrated significantly higher radioactivities than HMPAO ($F(1, 10) = 26.5$, $p < 0.001$, two-way ANOVA: tracer by region). On the other hand, in the cerebral cortex, except for the medial aspect of the parieto-occipital region, there were no significant differences between the two ($F(1, 50) = 1.90$, two-way ANOVA: tracer by region).

To compare the SPECT images with the PET images, ratios were calculated using ROI values. The gray matter/white matter ratios with HMPAO (1.47) and ECD (1.52) were significantly lower than the rCBF-PET (2.72) [Student's t-test: $p < 0.001$ after correction of multiple comparisons (*19*)]. Similarly, the cerebral cortex/cerebellum and insula/cerebral cortex ratios with rCBF-PET (1.04 and 1.32, respectively) were significantly higher than with HMPAO (0.88 and 1.09) or ECD (0.87 and 1.07) [Student's t-test: $p < 0.05$ and $p < 0.01$ after correction of multiple comparisons (*19*)]. The anterior cingulate/cerebral cortex RI concentration ratio with rCBF-PET (1.10) was also significantly higher than the HMPAO value (0.92) [Student's t-test: $p < 0.05$ after correction of multiple comparisons (*19*)]. The medial aspect of the occipital gyrus/cerebral cortex ratio with ECD (1.29) was significantly higher than the HMPAO (1.13) and rCBF-PET (1.08) values [Student's t-test: $p < 0.01$ after correction of multiple comparisons (*19*)].

Figure 4 shows scatterplots of the overall correlation between radioactivity of HMPAO or ECD, globally normalized to 50 counts/voxel, and rCBF measured with ^{15}O-butanol PET for each voxel. A curvilinear relationship is demonstrated, underestimations of HMPAO and ECD being observed in high flow regions and overestimations in low regions.

DISCUSSION

This human SPECT study specifically concentrated on normal cerebral perfusion pattern with HMPAO and ECD using an anatomical standardization technique. As a result we could identify marked differences between agents with higher uptakes in the cerebellum and the basal ganglia in the HMPAO case and in the medial aspect of the occipital lobe with ECD.

In this study, a relatively small number of subjects was used for each tracer due to ethical considerations and equipment restrictions in the institute. Previous PET studies (*20,21*) demonstrated, however, that there is no significant inaccuracy in rCBF patterns when PET data are obtained from at least six individuals. Therefore, the data generated in this study can be regarded as reproducible with minimal variability.

Our results of ROI analysis were consistent with visual impressions of the images. The accuracy of the current anatomical standardization technique has a s.d. of approximately 3 mm (*22*). Therefore, when considering the resolution power of the SPECT apparatus, it can be stated that the ROIs were drawn for the same anatomical structures in all subjects.

Also in this study, a coefficient of 0.1 was used for attenuation correction of all SPECT measurements. If another coefficient value, such as 0.11 or 0.12, is used, the ratio of counts

between internal structures in the brain can be altered. The difference between SPECT and PET attenuation correction algorithms can influence the ratio of counts between internal brain structures.

Each SPECT scan was performed 5–10 min after ^{99m}Tc-HMPAO injection or ^{99m}Tc-ECD. It has been described that ^{99m}Tc-HMPAO levels throughout the brain reach a maximum at 1 min postinjection, followed by some loss of material and plateau by 2 min (*1*). The brain uptake of ^{99m}Tc-HMPAO decreases faster than ^{99m}Tc-ECD (*23*). Whole brain time-activity curves of ^{99m}Tc-ECD demonstrate a rapid rise after the tracer injection and a plateau 3 min postinjection. On the other hand, the intracranial background activity was found to be unchanged during the whole brain periods, while the extracranial background activity reduced with time (*24,25*). These results suggested that brain SPECT data acquisition with ^{99m}Tc-ECD can safely be initiated 5 min postinjection (*24*). This is the rationale for our timing of 5–10 min postinjection. Although in this study, relatively early images postinjection could contain tracer activities in the vascular compartment within the brain.

Glutathione may be important for the in vivo conversion of ^{99m}Tc-HMPAO to hydrophilic forms with involvement in the mechanism of trapping in brain and other cells (*26*). On the other hand, selective retention in brain and rapid blood elimination and renal excretion of ECD are due to variation in its metabolic transformation to polar end products (*27*). Hydrolysis of ECD may be performed chemically and enzymatically by many different enzyme systems (*28*). Therefore, we speculate that the differences in cerebral perfusion pattern observed between the two agents are mainly due to variation in the mechanisms responsible for their cerebral accumulation.

We found higher radioactivities in the cerebellum and basal ganglia in the HMPAO-SPECT images, in line with the previous report (*29,30*). This disproportionately high uptake could be due to the higher capillary density than in most forebrain structures (*31*). Alternatively, biochemical characteristics of the tracer rather than flow of blood might be important (*29*). In the ECD-SPECT images, however, the regional distribution ratio of the cerebral cortex compared with the cerebellum was almost the same as in the HMPAO case.

In the ECD-SPECT images, higher radioactivities were observed in the medial aspect of the occipital lobe, especially in the cortex lining the calcaline sulcus, that is, the primary visual cortex. Occipital radioactivities were earlier described to be significantly higher with ECD than with HMPAO (*5*). The biochemical reason for this remains unclear. Rockel et al. (*32*) have reported that, with the exception of area 17 in the visual cortex in several primates, the same absolute numbers of neurons have been found in all areas and all mammalian species. In the binocular part of area 17 in primates there are approximately 2.5 times more neurons. Moreover, ^{123}I-iomazenil, which binds to the central benzodiazepine receptor found exclusively in the membrane of neurons, also shows the highest uptake in the occipital region (*33*). Thus, the distribution of ECD in the brain may be related to the density of neurons.

Both HMPAO-SPECT and ECD-SPECT resulted in underestimation of high rCBF. This may be due to a limited first-pass extraction fraction at the blood-brain barrier and back-diffusion from brain to blood that is related to the accumulation of both agents in the brain. This may also have caused the lower gray matter/white matter radioactivity ratios with HMPAO and ECD. On the other hand, both HMPAO-SPECT and ECD-SPECT demonstrated overestimation of lower rCBF regions, presumably due to a lower resolution or more scattered photons than in the case with PET. The overestimation of lower rCBF regions by HMPAO and ECD also may be related to the kinetics of these tracers compared to another tracer such as ^{123}I-IMP (*34*). Therefore, we conclude that neither HMPAO-SPECT nor ECD-SPECT images directly reflect rCBF. As the specific patterns of each agent's accumulation could not be corrected by quantitation and linearization procedures, this anomaly should be taken into consideration when making clinical diagnoses from SPECT images.

This study demonstrates a normal database for which we generated mean and the s.d. We believe that the data are necessary as a background to clinical diagnoses. This study was not intended to estimate clinical usefulness or behavior as indices of change in perfusion with each agent.

CONCLUSION

Generation of anatomically standardized SPECT images from normal subjects using HMPAO and ECD demonstrated clear differences in their RI accumulation patterns. This variation must be considered in making clinical diagnoses from SPECT images.

ACKNOWLEDGMENTS

We thank Professor Roland, Kalorinska Institute, Stockholm, for the use of the PET images. A part of this study was supported by a Grant-in-Aid for Scientific Research (05454297) from the Japanese Ministry of Education, Science, Sports and Culture and Research Grant for Aging and Health, from Japanese Ministry of Health and Welfare.

REFERENCES

1. Sharp PF, Smith FW, Gummell HG, et al. Technetium-99m HMPAO stereoisomers as potential agents for imaging regional cerebral blood flow: human volunteer studies. *J Nucl Med* 1986;27:171–177.
2. Léveillé J, Demonceau G, De Roo M, et al. Characterization of technetium-99m-L,L-ECD for brain perfusion imaging, part 2: biodistribution and brain imaging in humans. *J Nucl Med* 1989;30:1902–1910.
3. Vallabhajosula S, Zimmerman RE, Picard M, et al. Technetium-99m-ECD: a new brain imaging agent: in vivo kinetics and biodistribution studies in normal human subjects. *J Nucl Med* 1989;30:599–604.
4. Shishido F, Uemura K, Inugami A, et al. Discrepant ^{99m}Tc-ECD images of CBF in patients with subacute cerebral infarction: a comparison of CBF, CMRO2 and ^{99m}Tc-HMPAO imaging. *Ann Nucl Med* 1995;9:161–166.
5. Huglo D, Rousseaux M, Steinling M. Comparison of semiquantitative regional cerebral uptake of ^{99m}Tc-ECD and ^{99m}Tc-HMPAO using SPECT. *Circulation et Métabolisme du Cerveau* 1994;11:231–245.
6. Claus JJ, Harskamp F, Breteler MMB, et al. The diagnostic value of SPECT with ^{99m}Tc-HMPAO in Alzheimer's disease: a population-based study. *Neurology* 1994; 44:454–461.
7. Suess E, Malessa S, Ungersböck K, et al. Technetium-99m-d,l-HMPAO uptake and glutathione content in brain tumors. *J Nucl Med* 1991;32:1675–1681.
8. Zubal IG, Spencer SS, Imam K, et al. Difference images calculated from ictal and interictal technetium-99m-HMPAO SPECT scans of epilepsy. *J Nucl Med* 1995;36: 684–689.
9. Ito H, Kawashima R, Awata S, et al. Hypoperfusion in the limbic system and prefrontal cortex in depression: a SPECT study using an anatomical standardization technique. *J Nucl Med* 1996;37:410–414.
10. Jacobs A, Put E, Ingels M, Bossuyt A. Prospective evaluation of technetium-99m-HMPAO SPECT in mild and moderate traumatic brain injury. *J Nucl Med* 1994;35: 942–947.
11. Roland PE, Graufelds CJ, Wahlin J, et al. Human brain atlas for high-resolution function and anatomical mapping. *Hum Brain Mapping* 1994;1:173–184.
12. Hatta T, Nakatsuka Z. Handedness inventory. In: Ohno D, ed. *Papers on celebrating 63rd birthday of Professor Ohnishi*. Osaka, Japan: Osaka City University; 1975:224–245.
13. Kimura K, Hashikawa K, Etani H, et al. A new apparatus for brain imaging: four-head rotating gamma SPECT. *J Nucl Med* 1990;31:603–609.
14. Budinger TF, Gullberg GT, Huesman RH. *Image reconstruction from projections*. Herman GT, ed. New York: Springer-Verlag; 1979:197.
15. Chang LT. Attenuation correction and incomplete projection in SPECT. *IEEE Trans Nucl Sci* 1979;26:2780–2789.
16. Chang LT. A method for attenuation correction in radionuclide computed tomography. *IEEE Trans Nucl Sci* 1978;25:638–643.
17. Bergström M, Boethius J, Erikson L, Greiz T, Ribbe T, Widén L. Head fixation device for reproducible position alignment in transmission CT and positron emission tomography. *J Comput Assist Tomogr* 1981;5:136–141.
18. Roland PE, Levine B, Kawashima R, Åkerman S. Three-dimensional analysis of clustered voxels in ^{15}O-butanol brain activation images. *Hum Brain Mapping* 1993;1:3–19.

19. Dunnett CW. New table for multiple comparisons with a control. *Biometrics* 1964;20:482–491.
20. Fox PT, Mintun MA, Reiman EM, Raichle ME. Enhanced detection of focal brain responses using intersubject averaging and change-distribution analysis of subtracted PET images. *J Cereb Blood Flow Metab* 1988;8:642–653.
21. Watson JDG, Myers R, Frackowiak RSJ, et al. Area V5 of the human brain: evidence from a combined study using positron emission tomography and magnetic resonance imaging. *Cereb Cortex* 1993;3:79–94.
22. Koyama M, Kawashima R, Ito H, et al. Normal cerebral perfusion of ^{99m}Tc-HMPAO brain SPECT: evaluation by an anatomical standardization technique. *Jpn J Nucl Med* 1995;32:969–977.
23. Léveillé J, Botez MI, Taillefer R, et al. A clinical comparison of ^{99m}Tc-HMPAO and ^{99m}Tc-ECD in normal volunteers and patients as brain perfusion imaging agent [Abstract]. *J Nucl Med* 1988;29:844.
24. Ueda O, Ashihara T, Wake S, et al. Temporal change in regional brain distribution of the technetium-99m-ethyl cysteinate dimer. *Jpn J Radio Technol* 1993;49:1609–1615.
25. Léveillé J, Demonceau G, Walovitch RC. Intrasubject comparison between technetium-99m-ECD and technetium-99m-HMPAO in healthy human subject. *J Nucl Med* 1992;33:480–484.
26. Neirinckx RD, Bruke JF, Harrison RC, Forster AM, Andersen AR, Lassen NA. The retention mechanism of technetium-99m-HMPAO: intracellular reaction with glutathione. *J Cereb Blood Flow Metab* 1988;8:S4–S12.
27. Walovitch RC, Franceschi M, Picard M, et al. Metabolism of ^{99m}Tc-L,L-ethyl cysteinate dimer in healthy volunteers. *Neuropharmacology* 1990;30:283–292.
28. Borman G, Van Nerom C, Hoogmartens M, DeRoo M, Verbruggen A. Metabolism of ^{99m}Tc-ECD in isolated rat organs. *J Nucl Med* 1989;30:743.
29. Isaka Y, Iiji O, Imaizumi M, Ashida K, Itoi Y. Quantification of regional cerebral blood flow using ^{99m}Tc-HMPAO SPECT and intravenous ^{133}Xe injection method. *Jpn J Nucl Med* 1992;29:1463–1473.
30. Syed GMS, Eagger S, Toone BK, Levy R, Barrett JJ. Quantification of regional cerebral blood flow using ^{99m}Tc-HMPAO and SPECT: choice of the reference region. *Nucl Med Comm* 1992;13:811–816.
31. Heiss WD, Herholz K, Podreka I, Neubauer I, Pietrzyk U. Comparison of [^{99m}Tc]HMPAO SPECT with [^{18}F]fluoromethane PET in cerebrovascular disease. *J Cereb Blood Flow Metab* 1990;10:687–697.
32. Rockel AJ, Hiorns RW, Powell TPS. The basic uniformity in structure of the neocortex. *Brain* 1980;103:221–244.
33. Abi-Dargham A, Laruelle M, Seibyl J, et al. SPECT measurement of benzodiazepine receptors in human brain with iodine-123-iomazenil: kinetic and equilibrium paradigms. *J Nucl Med* 1994;35:228–238.
34. Nakano S, Kinoshita K, Jinnouchi S, Hoshi H, Watanabe K. Comparative study of regional cerebral blood flow images by SPECT using xenon-133, iodine-123-IMP and technetium-99m-HMPAO. *J Nucl Med* 1990;30:157–164.

Discrepancies Between HMPAO and ECD SPECT Imaging in Brain Tumors

J.-P. Papazyan, J. Delavelle, P. Burkhard, P. Rossier, C. Morel, B. Maton, P. Otten, G.P. Pizzolato, D.A. Rüfenacht and D.O. Slosman
Division of Nuclear Medicine, Neuroradiology Unit, Clinics of Neurology and Neurosurgery and Neuropathology Unit, Geneva University Hospital, Geneva, Switzerland

Among several brain radiopharmaceuticals for SPECT imaging, ^{99m}Tc complexes of HMPAO and ECD are the most widely used. They are considered to be equal in their capacity to reflect regional cerebral blood flow; but discrepancies between HMPAO and ECD brain uptake have been reported in stroke patients. This paper reports our observations regarding discrepancies between HMPAO and ECD SPECT in 14 of 23 patients with suspected brain tumors or presumed metabolic cerebral abnormalities. We obtained similar conflicting results, namely focal HMPAO hyperactivities and isoactive ECD SPECT. The majority of these discrepancies were found in patients with brain tumors (10 of 13 patients), while only 4 of the 10 remaining patients with nontumoral process showed similar discrepant results. The physiopathology behind these observations is discussed here, and it is likely to be related to the specific response to cellular metabolic disorders rather than to perfusion disturbances.

Key Words: brain perfusion; technetium-99m-HMPAO; technetium-99m-ECD; brain tumor

J Nucl Med 1997; 38:592–596

For more than a decade, several neutral and lipophilic brain radiopharmaceuticals have been developed to perform SPECT imaging of regional cerebral blood flow (rCBF) (*1*). Replacing the radioisotope ^{123}I with ^{99m}Tc gave investigators the capability to assess more easily rCBF in their own clinical environment. The ^{99m}Tc complex of hexamethylpropylene amine oxime (HMPAO), introduced in the late 1980s, showed rapid chemical decomposition, requiring its use within the first 30 min after reconstitution (*2,3*). This became a critical issue for epilepsy investigations during the ictal phase (*4*). Other ^{99m}Tc-labeled radiopharmaceuticals were then developed, in particular the ^{99m}Tc-ethylcisteinate dimer (ECD), which showed rapid in vivo blood clearance and prolonged in vitro stability (*5,6*). Moreover, in normal volunteers, intrasubject comparison between ECD and HMPAO showed better brain-to-background contrast with ECD than with HMPAO (*7*). Otherwise, HMPAO and ECD were considered to be similar with regard to their in vivo cerebral kinetics and initial distribution, as related to brain perfusion (*7*).

To our knowledge, the assessment of postischemic reperfusion was the only clinical situation in which HMPAO and ECD appeared to reflect rCBF in a different manner (*8,9*). Thus, in the present paper, we report our clinical experience of discrepant HMPAO and ECD brain uptake in several patients with suspected brain tumors or presumed metabolic cerebral abnormalities, and we discuss the possible physiopathological mechanisms behind these observations.

MATERIALS AND METHODS

We decided to perform both ECD and HMPAO-SPECT based on: (a) the results of our in vitro studies (*10,11*), (b) our preliminary discrepant observations related to decreased uptake of ECD associated to increased uptake of HMPAO and (c) a review of the literature. We made this decision under the following two conditions: (a) when the clinical suspicion was related to a possible situation of enhanced uptake of HMPAO (cerebral tumor, inflammatory or infectious processes and vascular disorders) and/or (b) when an increased uptake of HMPAO was observed in the first place.

During an 11-mo period (from March 1995 to February 1996), 234 brain SPECT examinations were executed in our division (34.6% patients were investigated for epilepsy, 32.9% with suspected or known brain tumors, 13.7% with cerebrovascular diseases and 18.8% with miscellaneous brain pathologies). Among our population, 23 patients (9 women, 14 men; mean age 60.2 yr, range 24–86 yr) underwent two consecutive brain SPECT exam-

Received Apr. 12, 1996; revision accepted Jul. 31, 1996.
For correspondence or reprints contact: Daniel Slosman, MD, Nuclear Medicine Division, Geneva University Hospital, 1211 Geneva 14 Switzerland.